Published in final edited form as:
J Mol Biol. 2007 January 12; 365(2): 513–522. doi:10.1016/j.jmb.2006.09.088.

Phage P22 procapsids equilibrate with free coat protein subunits

Kristin N. Parent, **Margaret M. Suhanovsky**, and **Carolyn M. Teschke***
University of Connecticut, Department of Molecular and Cell Biology, Storrs, CT

Abstract

Assembly of bacteriophage P22 procapsids has long served as a model for assembly of spherical viruses. Historically, assembly of viruses has been treated as a non-equilibrium process. Recently alternative models have been developed that treat spherical virus assembly as an equilibrium process. Here we have investigated whether P22 procapsids assembly reactions achieve equilibrium or are irreversibly trapped. To assemble a procapsid-like particle *in vitro*, pure coat protein monomers are mixed with scaffolding protein. Here we present data that show that free subunits can exchange with assembled structures, indicating that assembly is a reversible, equilibrium process. When empty procapsid shells (procapsids with the scaffolding protein stripped out) were diluted so that the concentration was below the dissociation constant (~5 μM) for coat protein monomers, free monomers were detected. The released monomers were assembly-competent; when NaCl was added to metastable partial capsids that were aged for an extended period, the coat subunits were able to rapidly re-distribute from the partial capsids and form whole procapsids. Lastly, radioactive monomeric coat subunits were able to exchange with the subunits from empty procapsid shells. The data presented here illustrate that coat protein monomers are able to dissociate from procapsids in an active state, that assembly of procapsids is consistent with reactions at equilibrium and follows the law of mass action.

Keywords

hysteresis; macromolecular assembly; icosahedral virus

Introduction

The amino acid sequence of viral capsid subunits must contain information about the structure of the subunits and the self-assembly process. The process of subunit assembly is strictly controlled through protein:protein interactions such that icosahedral structures are formed, rather than aberrant non-icosahedral structures. In addition, dsDNA viruses commonly assemble by first forming a precursor capsid that serves as a DNA packaging machine[1; 2; 3]. DNA packaging is accompanied by a conformational transition of the small round precursor capsid into a larger polyhedral DNA-containing capsid.

Phage P22 is an established model for the understanding of virus assembly where the assembly pathway involves a procapsid[4; 5; 6; 7; 8]. The morphogenic pathway of the dsDNA T=7 *Salmonella* bacteriophage P22 involves the co-assembly of 420 molecules of coat protein (product of gene 5; gp5) with 60–300 molecules of scaffolding protein (gp8) as well as some

*To whom correspondence should be addressed..

minor injection proteins (gp7, 16 and 20) and the portal protein complex (gp1) into a procapsid[9; 10]. Scaffolding protein directs procapsid assembly but is not found in mature phage. The dsDNA is actively packaged into the procapsid through the unique portal vertex[11], concomitant with DNA packaging, scaffolding protein exits from the procapsid to take part in additional rounds of assembly, and the capsid matures[12; 13]. None of the proteins are covalently modified or proteolyzed during folding, assembly or maturation.

An important advantage of phage P22 as an assembly model is the simplicity of the system. The proteins needed for assembly of P22 procapsid-like particles can be purified and are active for assembly[14]. *In vitro*, only coat and scaffolding proteins are required to assemble a procapsid-like particle, which we will refer to as a procapsid for simplicity[6; 15]. Both *in vivo* and *in vitro*, the number of scaffolding protein molecules incorporated into a procapsid varies, depending on the conditions of assembly[5; 16]. *In vitro* assembled procapsids have the same morphology and size as *in vivo* generated procapsids[6]. In addition, the product of the assembly reaction can be altered by changing the buffer conditions of the reaction[17]. In buffers with some salt added normal procapsids are assembled, while in the absence of salt metastable partial capsids form. We hypothesized that these are formed because the low salt solution increases the affinity of the interaction between coat and scaffolding protein, leading to over-nucleation. Over-nucleation causes depletion of the free coat protein so that complete capsids cannot be formed. The metastable partial capsids represent a true kinetic trap; the partial capsids are easily converted to normal procapsids by the addition of the appropriate concentration of salt. Therefore, *in vitro* assembly of P22 procapsids represents a simple yet elegant model for the *in vivo* assembly process.

Mathematical modeling of virus assembly has become a very active field. Some models focus on assembly of an individual particle[18; 19; 20; 21]. Other investigators are more interested in large populations, describing assembly in terms of micelles[22], crystals/filaments[23; 24] or spheres[25; 26]. All of these models agree on a few experimental observations of *in vitro* capsid assembly reactions: assembly kinetics are sigmoidal, there is unincorporated protein remaining at the end of the reaction, and capsids are very stable.

P22 procapsid assembly was described some years ago in terms of a classical polymerization reaction[8]. The experimental approach was groundbreaking and represented the first time such an effort was undertaken for capsid assembly. Prevelige *et al.*, 1993[8], described P22 procapsid assembly reactions as unidirectional or irreversible, and therefore not at equilibrium. In classical polymerization, the protein left at the end of an assembly reaction marks the “critical concentration” in stochastic equilibrium with the polymer, and is required to maintain it[8; 23; 24; 27]. Diluting the polymer results in dissociation to maintain this critical concentration[23; 27]. However, models of polymerization that are specific to spherical polymers of defined size (i.e. capsids) have since been developed. For spherical particles of defined size (n), the law of mass action, $K=[\text{capsid}]/[\text{subunit}]^n$, implies that below some concentration there will be little or no capsid, and above that concentration almost all additional protein will assemble leaving behind a pseudo-critical concentration[28; 29]. In simulations, assembly reactions of spheres closely approaches the equilibrium calculated from the known affinity of subunit-subunit interactions of capsids[19; 28; 29; 30], suggesting that analysis of capsid assembly based on the law of mass action is a reasonable method for understanding these complex reactions.

There is a current dispute over whether a capsid assembly reaction reaches equilibrium and is therefore able to dissociate, or if the reaction is irreversible. In some cases, a reversible reaction can appear irreversible when the dissociation reaction is slow compared to the forward association reaction, a phenomenon called hysteresis. Hysteresis is relatively common in folding and unfolding reactions of multi-subunit assemblies[31]. Generally, hysteresis in protein folding is observed as the requirement for high concentrations of denaturant to unfold a

complex but that urea concentration completely inhibits reassembly; a much lower denaturant concentration is required to refold and assemble the complex. However, if a reaction displays hysteresis, it does not mean that such a reaction is not at equilibrium[32; 33]. Often if the reaction is incubated for long enough times, the apparent hysteresis disappears, with unfolding transitions eventually converging with those of refolding. Hysteresis for capsid dissociation, which is caused by the high kinetic energy barrier to disassembly, occurs because capsids do not have any frayed ends to initiate dissociation[34]. For capsids, this means dissociation in an experimentally convenient time frame usually requires high amounts of a denaturant or high pressure[34; 35; 36]. Here we directly test the idea of whether P22 procapsid assembly reactions can equilibrate with free subunits, even in the face of the hysteresis of assembly reactions.

Results

Coat protein dissociates from procapsids

We recently determined the approximate average subunit dissociation constants for coat and scaffolding protein to be 5 μM and 28 μM, respectively[37]. Previous investigators have established that scaffolding protein is readily able to equilibrate between free and procapsid-bound pools[38; 39]. If assembled coat protein can also equilibrate with free subunits as expected for reactions at equilibrium, then when the assembled particles are diluted below the K_d values for monomer association, monomers should be present by the law of mass action. In this experiment, empty procapsid shells were used. Empty procapsid shells are procapsids stripped of most of their scaffolding protein. Since empty procapsid shells have only a residual amount of scaffolding protein, quantification of small amounts of coat protein monomers was made easier, while still allowing us to observe that scaffolding protein equilibrates as previously observed (data not shown).

Solutions of empty procapsid shells comprised of WT coat protein were diluted to ~5 and 0.5 μM (in monomer concentration; 0.012 and 0.0012 μM shells) and incubated at 4, 20, 37, and 41 °C for increasing times. In addition, a ~ 5 μM solution of shells comprised of a coat protein variant, F353L, was also investigated. We chose to include the F353L variant in this study since it dissociates more readily than WT. In this experiment, no significant loss of protein due to precipitation or non-specific adsorption was found even after 7 days incubation (data not shown). Data for F353L shells incubated at 41 °C are not shown because the protein was aggregation-prone at the longer incubation times. Aliquots of each sample were applied to a linear 5–20% sucrose gradient to separate shells from monomeric subunits. After centrifugation the gradients were fractionated and the fractions analyzed on SDS gels, which were silver stained. A representative pair of gels for the F353L variant are shown in Figure 1A. The top panel shows that prior to incubation, all of the coat protein migrates as shells, with no free monomer apparent. In the bottom panel, monomeric proteins are easily visualized even after one day of incubation at 37 °C.

The amount of coat protein in the position of monomer and shells for each type of protein and for each sample was quantified by densitometry (Figure 1B). The fraction of WT or F353L coat protein that sediments in the monomer position is shown as a function of time at four temperatures, from two separate experiments. Even after one day, coat monomers were easily visualized in each of the protein concentrations for shells of WT and F353L coat proteins, especially at temperatures above 20 °C. At a tenfold lower protein concentration, a greater fraction of WT coat protein monomers was released and also followed a similar temperature-dependence (data not shown). The destabilizing amino acid substitution, F353L, caused a greater release of coat protein monomer as compared to WT coat protein. Although in this experiment we have not achieved complete dissociation, consistent with the hysteresis observed in capsid assembly reactions[8; 34], the observable dissociation of the shells followed concentration, time-, and temperature-dependence, which are characteristic of reactions that

can reach equilibrium. These data are consistent with the hypothesis that these particles follow the law of mass action.

The entire population of coat protein monomers is assembly-competent

Above, we demonstrated that coat subunits dissociated from empty procapsid shells. Next we determined if these free coat protein subunits are assembly-competent or if they remain as free subunits simply because they were not able to re-assemble.

Because the concentration of the monomeric subunits is below the critical concentration for assembly, we used an alternative technique to determine if released subunits are assembly-competent. In low concentrations of NaCl and when scaffolding protein is in excess to coat protein, assembly results in metastable partial capsids[17]. These partial capsids remain in this metastable state until either NaCl is added or more coat protein. Partial capsids were used here to determine if coat protein held for extended periods could remain assembly-competent.

In Figure 2A, partial capsids were assembled with WT coat protein and the products were run on sucrose gradients and quantified as described above. We found that >95% of coat protein in the sample was consumed in a reaction that generates partial structures, whereas in an assembly reaction performed with salt present at the start of the reaction, only ~35 % of the coat protein is consumed as procapsids (Figure 2B). If salt is added to partial structures after ~20 hours, the partial structures rapidly redistribute and a greater number of procapsids are produced when compared to reactions that had salt present at the start. These data show that essentially all of the coat protein in our assembly reactions is competent. Although we cannot conclusively show that the released subunits from the partial structures are able to nucleate, they are clearly competent for elongation. Therefore, it is likely that the residual coat protein monomers left after a normal procapsid assembly reaction is due to the pseudo-critical concentration, below which assembly does not occur[28], and not due to the inability of the remaining monomers to assemble.

When NaCl is added to partial capsids, there is a rapid increase in the light scattering in response to the formation of complete procapsids (Figure 2C). Note that there is no decrease in the light scattering intensity prior to the rapid rise in intensity upon addition of NaCl. This observation suggests that all of the partial capsids do not need to completely dissociate in order to form whole procapsids. Rather, some partial capsids dissociate while concomitantly other partial capsids assemble to procapsids. Negative stain electron micrographs taken at varying times during re-distribution of the subunits are consistent with this result (data not shown). These data indicate that once released from partial capsids, coat protein monomers are still able to assemble, even after extended aging in the partial structures.

Partial capsids have similar stability to procapsids

An argument could be made that the coat subunits released from partial capsids are assembly-competent monomers because partial capsids must be less stable than procapsids or empty procapsid shells, or have a different conformation. In order to determine the relative stabilities of partial capsids to procapsids, urea titrations of partial capsids and *in vitro* assembled procapsids were done.

Each type of particle was incubated in 0 – 7.6 M buffered urea. The samples were incubated for ~ 20 hours and the resulting light scattering at 500 nm was measured (Figure 3). Shown is data that were normalized so that the highest signal was set to 1 and the lowest to 0. In the inset panel is the raw light scattering data. There are two transitions seen in the data. From 0 – ~2 M urea, scaffolding protein is extracted from the particles[40]. Another transition is observed between ~3 – 6 M urea, which represents the disassembly and denaturation of coat protein

from the particles[35; 40]. The midpoint ($C_{1/2}$) of the first transition is ~ 1.2 M urea for procapsids and ~ 1.1 M urea for partial capsids, which are not significantly different. This result suggests that within these particles, scaffolding protein is bound with about the same affinity, i.e., to about the same interaction site. Our data indicate that during nucleation, the binding between scaffolding and coat proteins is tight in low salt, but during elongation, the affinity may be similar in high and low salt.

The $C_{1/2}$ of the second transition is ~ 4.8 M urea for *in vitro* assembled procapsids and ~ 4.4 M urea for partial capsids, indicating that the partial capsids dissociate at a marginally lower urea concentration than procapsids. Urea titrations of *in vivo* assembled procapsids showed similar stability in urea as the *in vitro* assembled procapsids (data not shown). The slight change in transition midpoint between partial capsids and complete procapsids suggests that the strength of coat protein subunit interaction in the two types of particles is not significantly different.

Urea titrations of empty procapsid shells of the F353L coat protein were compared to shells comprised of WT coat protein (data not shown). The midpoint of the transition for the F353L curve occurred at ~ 3.6 M urea, which is significantly destabilized when compared to the $C_{1/2}$ for shells comprised of WT coat protein, which occurred at ~ 4.8 M urea. These data are consistent with the data presented in Figure 1, where shells assembled with F353L coat protein dissociate more readily under native conditions when compared to shells comprised of WT coat protein.

Monomeric subunits exchange with shells

Our data suggest that coat protein subunits can dissociate from assembled structures in an assembly-competent conformation. If this is the case and capsids are in stochastic equilibrium with free coat protein monomers, then these free subunits should exchange with assembled structures. Radioactively labeled coat protein monomers at ~ 0.5 μM final concentration were mixed with non-labeled empty procapsid shells at 0.006 or 0.012 μM and were incubated at either 20 or 41 °C for one day. Monomeric subunits were separated from shells via sucrose gradient sedimentation, as described above, and the fractions were analyzed by liquid scintillation counting. The percent of radioactively labeled proteins in monomers or assembled structures in the sucrose gradient was determined and is shown in Figure 4. When the concentration of shells was higher, a greater fraction of the labeled coat protein monomers transferred as compared to the lower concentration of shells. This result shows the expected concentration dependence of the dissociation reaction, and is consistent with the law of mass action. That is, when the shells are more dilute, they dissociate more readily leading to less exchange. Also, a higher percent of transfer was seen at 20 °C, as compared to 41°C. This result is consistent with our earlier experiments (Figure 1) where a greater dissociation of subunits occurs at higher temperatures. The observation of subunit exchange is consistent with a reaction that equilibrates, where free subunits are in exchange with assembled structures.

Discussion

Here we have asked if capsid assembly reactions reach equilibrium, using phage P22 procapsid assembly as our model. P22 procapsid formation is an excellent model to answer this question because there are no covalent modifications to the proteins once assembled. Indeed, we have recently characterized the thermodynamics of the assembly reaction and found that procapsid assembly is driven by weak subunit interactions but the assembled structure is stable because of the large number of multivalent subunits that comprise a procapsid[37].

In vitro assembly of P22 procapsids

P22 procapsid assembly was previously described in terms of a classical polymerization reaction for filamentous structures[8]. Using this model, Prevelige *et al.*, 1993 described P22 procapsid assembly reactions as irreversible (kinetically trapped) and not at equilibrium. In contrast, here we have observed that procapsids will disassemble when at low enough concentrations and given enough time, an observation incompatible with irreversible procapsid assembly and consistent with assembly reactions that are able to achieve equilibrium. The observation that free subunits can exchange with assembled structures is consistent with the ability of viral capsid subunits to breathe[34; 41] and ultimately could be related to capsid expansion. Subunit exchange also suggests that prior to assembly completion, dissociation of subunits is possible, which would allow for thermodynamic proofreading to ensure that only correctly folded subunits are incorporated[42].

A true kinetic trap can be observed for P22 assembly in low NaCl solution conditions[17]. These reactions consume all of the subunits. If NaCl is added to the trapped partial capsids, the subunits rapidly re-distribute to form procapsids; thus, the released subunits are assembly-competent, even after incubation for weeks. Importantly, the high reversibility suggests that dissociation and assembly reactions follow similar paths. This experiment also indicates that the subunits not consumed at the end of a normal assembly reaction are not incompetent, but remain because there are not enough subunits left to support continued assembly, perhaps because the concentration of free subunits may fall below the concentration required to form a nucleation complex. Thus, proper procapsid assembly produces the predicted pseudo-critical concentration for reactions at equilibrium[25;43].

Hysteresis in assembly reactions

Capsid assembly reactions are characterized by a few key observations[28]. One is that the reactions display hysteresis between assembly and disassembly because of the high energetic barrier to disassembly[34]. Hysteresis is often seen in association reactions of large, multi-domain proteins such as bacterial luciferase[33], transthyretin[32], creatine kinase[44], and collagen[45]. All of these examples are marked by high kinetic energy barriers to complex dissociation, which prevent coincidence of unfolding/folding transitions in experimentally convenient time scales; e.g., ~ a million years for the dissociation of bacterial luciferase.

Hysteresis has been observed for P22 procapsid assembly in previous experiments[35; 46]. We again observed hysteresis in the experiments described here; i.e., the expected dissociation of shells, based on the coat protein K_d[37], did not occur within the times examined.

Traditionally, capsid assembly reactions have been treated using classic nucleation theory[8; 23; 24; 27]. The nucleation model is inconsistent with the observation of hysteresis in capsid assembly reactions[28] because when equilibrium for a filamentous protein is reached, the rate of association of free subunits equals the rate of dissociation of subunits from the filament. Here we present data that indicates that P22 assembly is consistent with the more recent descriptions of capsid assembly reactions based on assembly of spheres[25] and molecular dynamics simulations of capsid assembly reactions, both of which predict hysteresis[19; 30]. The simulations displayed hysteresis even when the disassembly reaction was constrained to follow the same pathway as the forward reaction, a requirement of true equilibrium.

Virus assembly as a rule has been suggested to be irreversible[31], or in other words, the dissociation reaction does not occur. The concept of irreversibility will to some extent depend on the observation timescale. Here we see that capsids are able to dissociate on a long time scale; if one looked for subunit dissociation to occur on the scale of minutes, then capsid assembly might appear irreversible. Nevertheless, in the absence of irreversible post-assembly

transitions, such as seen with the cross-linking of capsid subunits in phage HK97[3], irreversibility is inconsistent with a pseudo-critical concentration, which is predicted from simulations, and is observed experimentally for phage P22 procapsids and the assembly of other viruses[37; 47; 48]. A pseudo-critical concentration is expected from capsid assembly reactions at equilibrium; in an irreversible assembly reaction all of the subunits would be consumed in the reaction.

A recent computer simulation method developed by Zhang and Schwartz (2006)[43] showed that capsid yield increases with the initial concentration of subunits. Conversely, the existence of kinetic traps significantly altered the concentration dependence for assembly so that capsid yield no longer showed any concentration dependence on initial subunit concentration. Results from this computer modeling support the observed P22 experimental data where procapsid production varied with input protein concentration, once above the pseudo-critical concentration[37]. Thus, the predicted concentration dependence directly supports P22 assembly as an equilibrium process, and not as an irreversible, kinetically trapped process, which would not show concentration dependence[43].

Comparison of in vivo versus in vitro assembly pathways

The *in vivo* assembly pathway of bacteriophage P22 has two major steps. The first step involves the co-polymerization of viral subunit proteins to form the precursor procapsid. The second step involves maturation of the procapsid upon DNA packaging. Maturation is considered to be an irreversible process, occurring as a result of a large energy input derived from DNA packaging, which is obligatory to overcome the high stability of the procapsid[40; 49]. *In vivo*, the entire phage biogenesis process is rapid, and occurs on a reasonable scale considering the life cycle of the host cell. For example at 30 °C, the protein synthesis, procapsid assembly and maturation steps occur in less than 70 minutes to produce a burst of infectious particles and lyse the host cell[50]. *In vivo*, the hysteresis that is apparent in an *in vitro* assembly reaction is not critical because of the irreversible nature of the capsid completion steps. However, since incorrect assemblies as well as coat protein aggregates are seldom observed during *in vivo* infections with wild-type phage[16; 51], thermodynamic proofreading is likely occurring, and would not be possible without subunit exchange.

During *in vitro* assembly, capsid maturation does not occur. Therefore, we can easily visualize whether or not procapsids dissociate and exchange with free subunits, given long enough time. The data presented here validate our recent work that characterized the thermodynamic contribution of the individual subunits[37] to procapsid assembly. Molecular modeling and a comprehensive biophysical characterization of the protein:protein interactions necessary for understanding the virus assembly process would not be possible studying the comparatively complicated *in vivo* pathway.

Collectively, our experimental data and the simulations of other investigators suggest that proper capsid assembly reactions do indeed reach equilibrium, albeit one with a high energy barrier to dissociation. The observed subunit exchange is inconsistent with the idea that procapsids are irreversibly trapped, but is consistent with procapsid assembly reactions that are able to equilibrate. In total, our findings suggest that equilibrium analysis[37; 52] based on the products of forward capsid assembly reactions provides a reliable methodology for understanding viral capsid assembly, even in light of the observed hysteresis in these reactions.

Materials and Methods

Refolded coat protein monomers

Purification of coat protein shells was performed as previously described[35]. Coat protein monomers were obtained from urea-denatured empty procapsid shells, as described previously, using dialysis at 4° C against 20 mM sodium phosphate buffer, pH 7.6. Monomers were spun at 175,000 x g at 4° C for 20 minutes to remove any aggregated or associated structures prior to *in vitro* assembly reactions. The assembly-competence of the monomers was evaluated using assembly reactions, described below.

Assembly reactions

To assemble partial structures, refolded coat protein monomers at a final concentration of 0.5 mg/mL (~11 μM) were mixed with scaffolding protein at 0.5 mg/mL (~18 μM) final concentration in 20 mM sodium phosphate buffer. Procapsids were assembled at the same protein concentrations, but the 20 mM sodium phosphate buffer was supplemented with 60 mM NaCl. The presence of partial or procapsid-like structures was confirmed by negatively stained electron micrographs as described previously[53; 54]. The progress of the reaction was followed by light scattering.

Light Scattering

Assembly reactions were monitored in a SLM Aminco-Bowman 2 spectrofluorometer at 20 ° C. The reaction was monitored by the increase in 90° light scattering at 500 nm with the bandpasses set to 4 nm. Two assembly reactions were done: 1) 60 mM NaCl final added ~20 hours after formation of the partial structures 2) extra 20 mM sodium phosphate buffer added ~20 hours after formation of the partial structures (to achieve the same final volume).

Dissociation reaction of shells

Empty procapsid shells composed of WT coat protein were diluted to 0.25, or 0.025 mg/mL (~5 and 0.5 μM monomer concentration, or 0.012 μM or 0.0012 μM shells, respectively) and shells composed of F353L coat protein were diluted to 0.25 mg/mL. The shells were diluted in 20 mM sodium phosphate buffer containing 1 mM PMSF, 10 μg/mL A-protinin, 10 μg /mL leupeptin, and 5 μg mg/mL pepstatin, and were incubated at 4, 20, 37, and 41 °C for up to 10 days in 5 mL polystyrene tubes (Fisherbrand) pretreated with Sigmacoat (Sigma). A sample of each reaction was applied to linear 5–20% sucrose gradients. The sedimentation was done at the experimental temperature, as described below. After centrifugation, the gradients were fractionated from the top into 100 μl fractions. The fractions were run on a 10% SDS-polyacrylamide gel and silver stained[55]. The coat protein bands were quantified using a Kodak EDAS system.

Sucrose gradient sedimentation

A sample of each reaction mixture was applied to the top of a 2.2 mL, linear 5 – 20% (w/w) sucrose gradient, prepared using a BioComp Gradient Master. The gradients were centrifuged in a Sorvall RCM120EX centrifuge with an RP55S rotor at 35,000 rpm for 55 min for samples at 4 °C, 35 min at 20 °C, 27 min at 37 °C, and 25 min at 41 °C. The protein content of each fraction was determined as described for each experiment.

Assembly-competence of released monomers

Assembly reactions were performed as described above to generate partial structures and procapsids, and were allowed to incubate at 20 °C for ~ 20 hours. The reactions were split, buffer was added to one sample, and NaCl was added to the other sample to a final concentration of 60 mM. 100 μl of each reaction mixture was applied to the top of a linear 5 – 20% sucrose

gradient, After centrifugation, the gradients were fractionated from the top into 100 μl fractions. The fractions were run on a 10% SDS-polyacrylamide gel and Coomassie stained. The coat protein bands were quantified using a Kodak EDAS system.

Urea titrations

Partial structures and procapsids were generated as described above, and held for ~48 hours at 20 °C. Samples were then diluted 1:5 into buffered urea, ranging 0 – 7.6 M and incubated at 20 °C for an additional ~ 20 hours. Light scattering of the resultant samples was monitored using a SLM Aminco-Bowman 2 spectrofluorometer, at 20 °C, using 90° light scattering at 500 nm with the bandpasses set to 4 nm. Fraction of signal was calculated by normalizing the light scattering at 0 M urea to a fraction remaining of 1, and setting the signal at 7.6 M urea to a fraction remaining of 0.

Analysis of subunit exchange

Radiolabeled coat protein was generated as described below and coat protein monomers were made as described above. The monomers at ~ 0.5 μM final concentration were mixed with non-labeled empty procapsid shells at ~ 0.006 μM or ~ 0.012 μM final shell concentration, and were incubated at either 20 or 41 °C for one day. Monomeric subunits were separated from shells via sucrose gradient sedimentation, as described above, and the fractions were analyzed by liquid scintillation counting. The difference of radioactivity sedimenting in the position of shells from two gradients, one with radioactive monomers that included the non-labeled shells and one with radioactive monomers alone, was used to calculate the percent transfer. The percent transfer was the fraction of total radioactivity that sedimented in the position of shells.

Purification of radiolabeled coat proteins

Overnight cultures were grown in minimal media (from a single isolated colony of DB7136 (hisC525^{-}am leu414^{-}am sup^{0}) at 37°C. Minimal media contains M9 plus 1 mM $MgSO_4$, 1 μM $FeCl_3$ and $CaCl_2$, 1.2% glucose, 0.008% leucine, 0.003% histidine. M9 media contains 1.28% $NaHPO_4$, 0.3% KH_2PO_4, 0.05% NaCl, and 0.1% NH_4Cl. The overnight cultures were used to inoculate a culture in minimal media, grown at 37°C. The cells were grown to a density of 3 x 10^8 cells/mL, and then infected with a multiplicity of infection of 17 with phage (3^{-}am, 13^{-}am) that were WT in all capsid proteins but were unable to package DNA or lyse cells. The infected cultures were grown for 45 minutes, followed by additions of 1.875 μCi/mL of [^{35}S]-methionine and [^{35}S]-cysteine protein labeling mix (10 mCi/mL, NEN Life Science Products) every 30 minutes for 3 hours and 45 minutes. The rest of the purification and scaffolding protein extraction was performed as described previously[35; 56].

Liquid Scintillation Counting

Individual fractions from the sucrose gradient sedimentation, as described above, were mixed at a 1:25 ratio with OptiFluor scintillation cocktail, and were measured in a Perkin Elmer 1450 Microbeta scintillation counter until each sample had reached 1% sigma accuracy of counting.

Acknowledgments

This work was supported by PHS grant GM053567 to CMT, a PHS fellowship GM073598 to KNP, and a University of Connecticut Research Foundation Grant. We also thank Adam Zlotnick for his enthusiasm and critical discussions regarding this project.

References

1. Heymann JB, Cheng N, Newcomb WW, Trus BL, Brown JC, Steven AC. Dynamics of herpes simplex virus capsid maturation visualized by time-lapse cryo-electron microscopy. Nat Struct Biol 2003;10:334–41. [PubMed: 12704429]
2. Earnshaw W, Hendrix R, King J. Structural studies of bacteriophage lambda heads and proheads by small angle X-ray diffraction. J Mol Biol 1980;134:575–594. [PubMed: 161330]
3. Duda RL, Hempel J, Michel H, Shabanowitz J, Hunt D, Hendrix RW. Structural transitions during bacteriophage HK97 head assembly. J Mol Biol 1995;247:618–35. [PubMed: 7723019]
4. Casjens S. Molecular organization of the bacteriophage P22 coat protein shell. J Mol Biol 1979;131:1–19. [PubMed: 385887]
5. Casjens S, Adams MB, Hall C, King J. Assembly-controlled autogenous modulation of bacteriophage P22 scaffolding protein gene expression. J Virol 1985;53:174–179. [PubMed: 3880825]
6. Fuller MT, King J. Regulation of coat protein polymerization by the scaffolding protein of bacteriophage P22. Biophys J 1980;32:381–401. [PubMed: 7018607]
7. Fuller MT, King J. Assembly *in vitro* of bacteriophage P22 procapsids from purified coat and scaffolding subunits. J Mol Biol 1982;156:633–665. [PubMed: 6750133]
8. Prevelige PE, Thomas D Jr, King J. Nucleation and growth phases in the polymerization of coat and scaffolding subunits into icosahedral procapsid shells. Biophys J 1993;64:824–835. [PubMed: 8471727]
9. King J, Botstein D, Casjens S, Earnshaw W, Harrison S, Lenk E. Structure and assembly of the capsid of bacteriophage P22. Philos Trans R Soc London B 1976;276:37–49. [PubMed: 13434]
10. Prevelige PE Jr, King J. Assembly of bacteriophage P22: a model for ds-DNA virus assembly. Prog Med Virol 1993;40:206–221. [PubMed: 8438077]
11. Bazinet C, King J. Initiation of P22 procapsid assembly *in vivo*. J Mol Biol 1988;202:77–86. [PubMed: 3262766]
12. Earnshaw W, Casjens S, Harrison SC. Assembly of the head of bacteriophage P22: x-ray diffraction from heads, proheads and related structures. J Mol Biol 1976;104:387–410. [PubMed: 781287]
13. Prasad BVV, Prevelige PE Jr, Marieta E, Chen RO, Thomas D, King J, Chiu W. Three-dimensional transformation of capsids associated with genome packaging in a bacterial virus. J Mol Biol 1993;231:65–74. [PubMed: 8496966]
14. Fuller MT, King J. Purification of the coat and scaffolding protein from procapsids of bacteriophage P22. Virology 1981;112:529–547. [PubMed: 7257185]
15. King J, Lenk EV, Botstein D. Mechanism of head assembly and DNA encapsulation in *Salmonella* phage P22 II. Morphogenetic pathway. J Mol Biol 1973;80:697–731. [PubMed: 4773027]
16. Parent KN, Ranaghan MJ, Teschke CM. A second site suppressor of a folding defect functions via interactions with a chaperone network to improve folding and assembly *in vivo*. Mol Microbiol 2004;54:1036–54. [PubMed: 15522085]
17. Parent KN, Doyle SM, Anderson E, Teschke CM. Electrostatic interactions govern both nucleation and elongation during phage P22 procapsid assembly. Virology 2005;340:33–45. [PubMed: 16045955]
18. Twarock R. A tiling approach to virus capsid assembly explaining a structural puzzle in virology. J Theor Biol 2004;226:477–82. [PubMed: 14759653]
19. Rapaport DC. Self-assembly of polyhedral shells: a molecular dynamics study. Phys Rev E Stat Nonlin Soft Matter Phys 2004;70:051905. [PubMed: 15600654]
20. Berger B, Shor PW, Tucker-Kellogg L, King J. Local rule-based theory of virus shell assembly. Proc Natl Acad Sci USA 1994;91:7732–6. [PubMed: 8052652]
21. Hemberg M, Yaliraki SN, Barahona M. Stochastic kinetics of viral capsid assembly based on detailed protein structures. Biophys J 2006;90:3029–42. [PubMed: 16473916]
22. McPherson A. Micelle formation and crystallization as paradigms for virus assembly. Bioessays 2005;27:447–58. [PubMed: 15770675]
23. Oosawa, F.; Asakura, S. Thermodynamics of the polymerization of protein. Academic Press; New York: 1975.

24. Zandi R, van der Schoot P, Reguera D, Kegel W, Reiss H. Classical nucleation theory of virus capsids. Biophys J 2006;90:1939–48. [PubMed: 16387781]
25. Endres D, Zlotnick A. Model-based analysis of assembly kinetics for virus capsids or other spherical polymers. Biophys J 2002;83:1217–30. [PubMed: 12124301]
26. Wales DJ. The energy landscape as a unifying theme in molecular science. Philos Transact A Math Phys Eng Sci 2005;363:357–75. [PubMed: 15664888]
27. Frieden C. Actin and tubulin polymerization: the use of kinetic methods to determine mechanism. Annu Rev Biophys Biophys Chem 1985;14:189–210. [PubMed: 3890879]
28. Zlotnick A. Theoretical aspects of virus capsid assembly. J Mol Recognit 2005;18:479–90. [PubMed: 16193532]
29. Schwartz R, Shor PW, Prevelige PE Jr, Berger B. Local rules simulation of the kinetics of virus capsid self-assembly. Biophys J 1998;75:2626–36. [PubMed: 9826587]
30. Hagan MF, Chandler D. Dynamic Pathways for Viral Capsid Assembly. Biophys J. 2006In press
31. Weber G, Da Poian AT, Silva JL. Concentration dependence of the subunit association of oligomers and viruses and the modification of the latter by urea binding. Biophys J 1996;70:167–73. [PubMed: 8770195]
32. Lai Z, McCulloch J, Lashuel HA, Kelly JW. Guanidine hydrochloride-induced denaturation and refolding of transthyretin exhibits a marked hysteresis: equilibria with high kinetic barriers. Biochemistry 1997;36:10230–10239. [PubMed: 9254621]
33. Sinclair JF, Ziegler MM, Baldwin TO. Kinetic partitioning during protein folding yields multiple native states. Nat Struct Biol 1994;5:320–6. [PubMed: 7664038]
34. Singh S, Zlotnick A. Observed hysteresis of virus capsid disassembly is implicit in kinetic models of assembly. J Biol Chem 2003;278:18249–55. [PubMed: 12639968]
35. Teschke CM, King J. Folding of the phage P22 coat protein *in vitro*. Biochemistry 1993;32:10839–10847. [PubMed: 8399234]
36. Foguel D, Teschke CM, Prevelige PE Jr, Silva JL. Role of entropic interactions in viral capsids: single amino acid substitutions in P22 bacteriophage coat protein resulting in loss of capsid stability. Biochemistry 1995;34:1120–1126. [PubMed: 7827060]
37. Parent KN, Zlotnick A, Teschke CM. Quantitative analysis of multi-component spherical virus assembly: Scaffolding protein contributes to the global stability of phage P22 procapsids. J Mol Biol 2006;359:1097–1106. [PubMed: 16697406]
38. Greene B, King J. Binding of scaffolding subunits within the P22 procapsid lattice. Virology 1994;205:188–197. [PubMed: 7975215]
39. Parker MH, Brouillette CG, Prevelige PJ. Kinetic and calorimetric evidence for two distinct scaffolding protein binding populations within the bacteriophage P22 procapsid. Biochemistry 2001;40:8962–70. [PubMed: 11467958]
40. Capen CM, Teschke CM. Folding defects caused by single amino acid substitutions in a subunit are not alleviated by assembly. Biochemistry 2000;39:1142–1151. [PubMed: 10653661]
41. Reisdorph N, Thomas JJ, Katpally U, Chase E, Harris K, Siuzdak G, Smith TJ. Human rhinovirus capsid dynamics is controlled by canyon flexibility. Virology 2003;314:34–44. [PubMed: 14517058]
42. Zlotnick A. Are weak protein-protein interactions the general rule in capsid assembly? Virology 2003;315:269–74. [PubMed: 14585329]
43. Zhang T, Schwartz R. Simulation study of the contribution of oligomer/oligomer binding to capsid assembly kinetics. Biophys J 2006;90:57–64. [PubMed: 16214864]
44. Zhu L, Fan YX, Zhou JM. Identification of equilibrium and kinetic intermediates involved in folding of urea-denatured creatine kinase. Biochim Biophys Acta 2001;1544:320–332. [PubMed: 11341941]
45. Engel J, Bachinger HP. Cooperative equilibrium transitions coupled with a slow annealing step explain the sharpness and hysteresis of collagen folding. Matrix Biol 2000;19:235–44. [PubMed: 10936448]
46. Prevelige PE Jr, King J, Silva JL. Pressure denaturation of the bacteriophage P22 coat protein and its entropic stabilization in icosahedral shells. Biophys J 1994;66:1631–1641. [PubMed: 8061212]

47. Zlotnick A, Johnson JM, Wingfield PW, Stahl SJ, Endres D. A theoretical model successfully identifies features of hepatitis B virus capsid assembly. Biochemistry 1999;38:14644–52. [PubMed: 10545189]

48. Zlotnick A, Aldrich R, Johnson JM, Ceres P, Young MJ. Mechanism of capsid assembly for an icosahedral plant virus. Virology 2000;277:450–6. [PubMed: 11080492]

49. Galisteo ML, King J. Conformational transformations in the protein lattice of phage P22 procapsids. Biophys J 1993;65:227–235. [PubMed: 8369433]

50. Aramli LA, Teschke CM. Single amino acid substitutions globally suppress the folding defects of temperature-sensitive folding mutants of phage P22 coat protein. J Biol Chem 1999;274:22217–22224. [PubMed: 10428787]

51. Lenk E, Casjens S, Weeks J, King J. Intracellular visualization of precursor capsids in phage P22 mutant infected cells. Virology 1975;68:182–199. [PubMed: 1103445]

52. Zlotnick A. To build a virus capsid. An equilibrium model of the self assembly of polyhedral protein complexes. J Mol Biol 1994;241:59–67. [PubMed: 8051707]

53. Thuman-Commike PA, Greene B, Malinski JA, King J, Chiu W. Role of the scaffolding protein in P22 procapsid size determination suggested by $T = 4$ and $T = 7$ procapsid structures. Biophys J 1998;74:559–568. [PubMed: 9449356]

54. Teschke CM, McGough A, Thuman-Commike PA. Penton release from P22 heat-expanded capsids suggests importance of stabilizing penton-hexon interactions during capsid maturation. Biophysical Journal 2003;84:2585–2592. [PubMed: 12668466]

55. Rabilloud T, Carpentier G, Tarroux P. Improvement and simplification of low-background silver staining of proteins by using sodium dithionite. Electrophoresis 1988;9:288–291. [PubMed: 2466660]

56. Prevelige PE Jr, Thomas D, King J. Scaffolding protein regulates the polymerization of P22 coat subunits into icosahedral shells *in vitro.* J Mol Biol 1988;202:743–757. [PubMed: 3262767]

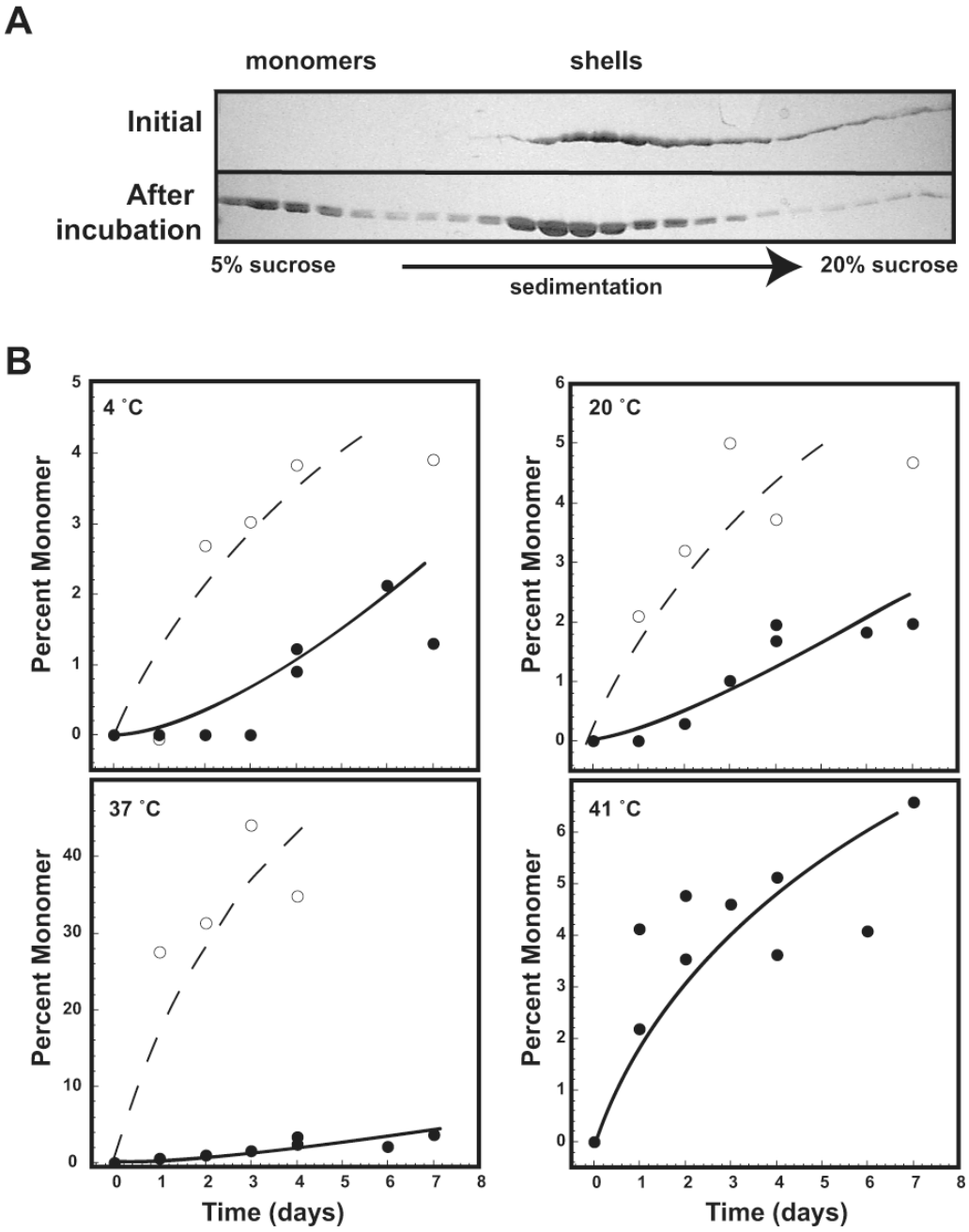

Figure 1. Phage P22 procapsid shells dissociate

Dilute solutions of P22 shells comprised of either WT or F353L coat proteins were incubated at 4, 20, 37, and 41 °C for times ranging immediately after dilution, up to a period of 7 days. The shells were separated from the monomeric subunits by sedimentation in a 5 – 20 % linear sucrose gradient. The fractions were run on SDS-PAGE, the gels were silver-stained, and the protein quantified by densitometry. In panel A, two representative gels are shown. The top panel is of shells comprised of F353L coat protein immediately after dilution, and the bottom panel is after a one day incubation at 37 °C. In panel B, densitometry data is shown for diluted WT (closed circles) and F353L shells (open circles), where the percent of protein found in the regions of the sucrose gradients where monomers sediment as a function of time is shown at

4, 20, 37 and 41 °C. Please note that different scales were used in these panels and the lines were drawn to aid the eye and do not represent a fit of the data to any model.

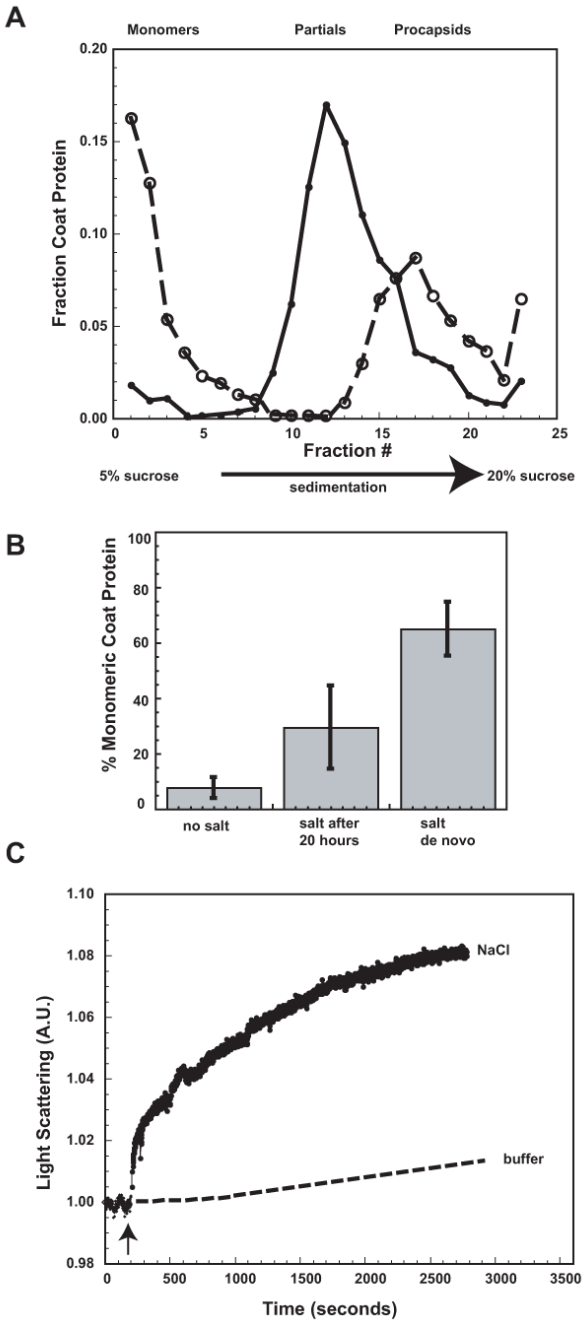

Figure 2. All phage P22 coat subunits are competent for assembly

Panel A shows densitometry profiles for partial capsids (closed circles, solid line) and *in vitro* assembled procapsids (open circles, dotted line) run on a 5 – 20 % linear sucrose gradient analyzed by SDS-PAGE, and Coomassie stained. Panel B represents the percent of subunits found where monomeric subunits sediment in a 5 – 20 % sucrose gradient (fractions 1 – 7) for reactions resulting in partial capsids (no salt), procapsids (salt de novo), and procapsids formed after salt was added to partial structures (salt after 20 hours). Panel C represents light scattering data, where salt (closed circles, solid line) and buffer (dotted line) was added to partial structures. The arrow shows the time of NaCl addition.

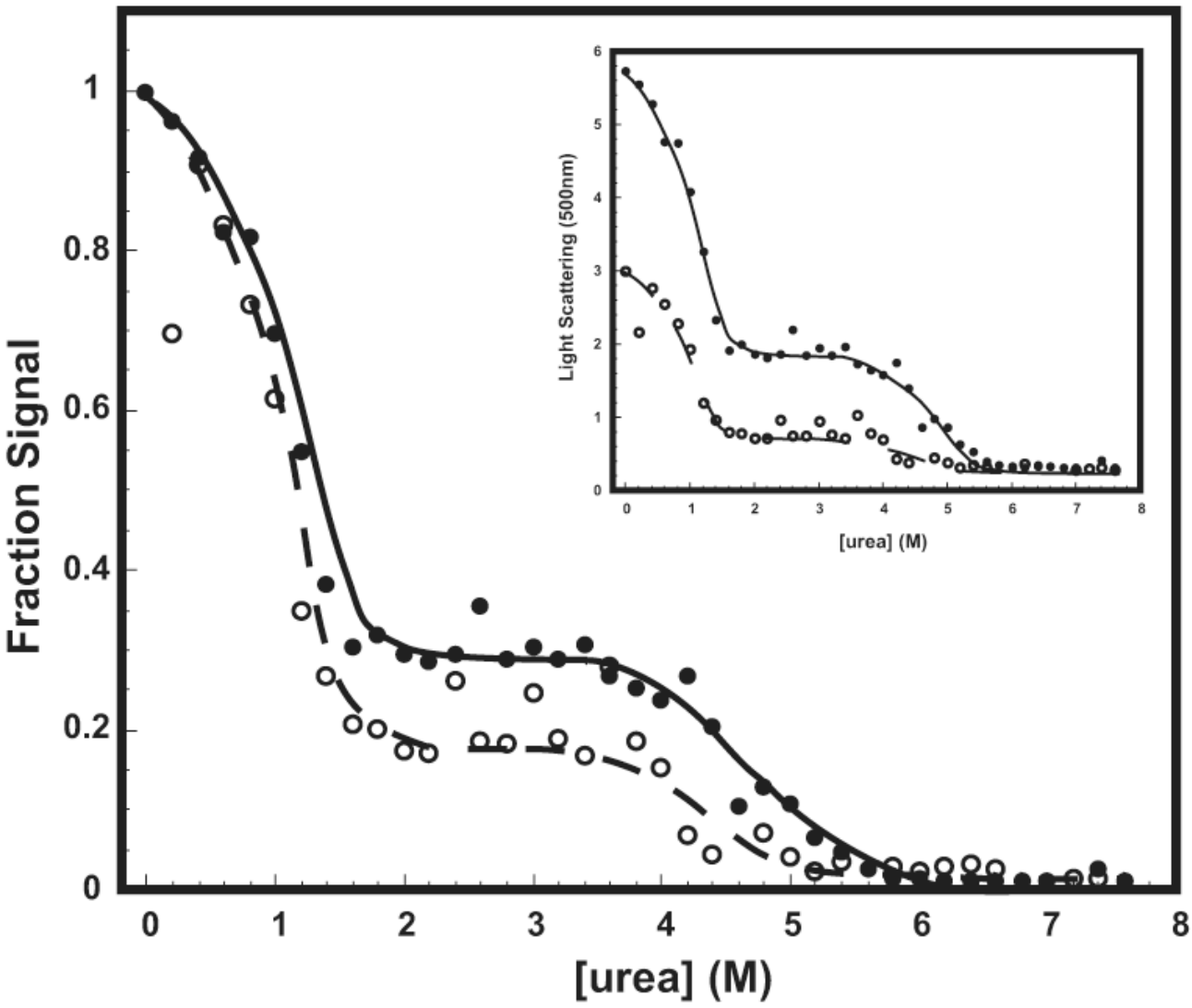

Figure 3. Partial structures and procapsids have similar stability

Urea titrations were performed with partial structures (open circles) and *in vitro* assembled procapsids (closed circles) incubated in buffered urea ranging 0 – 7.6 M. The fraction remaining represents data normalized to the highest signal in 0 M urea set to a value of 1.0, and the signal at 7.6 M urea set to 0.0 The inset shows the raw light scattering data, where the partial capsids show the expected lower light scattering compared to procapsids. The lines were drawn to aid the eye and are not meant to represent the fit of the data to any model.

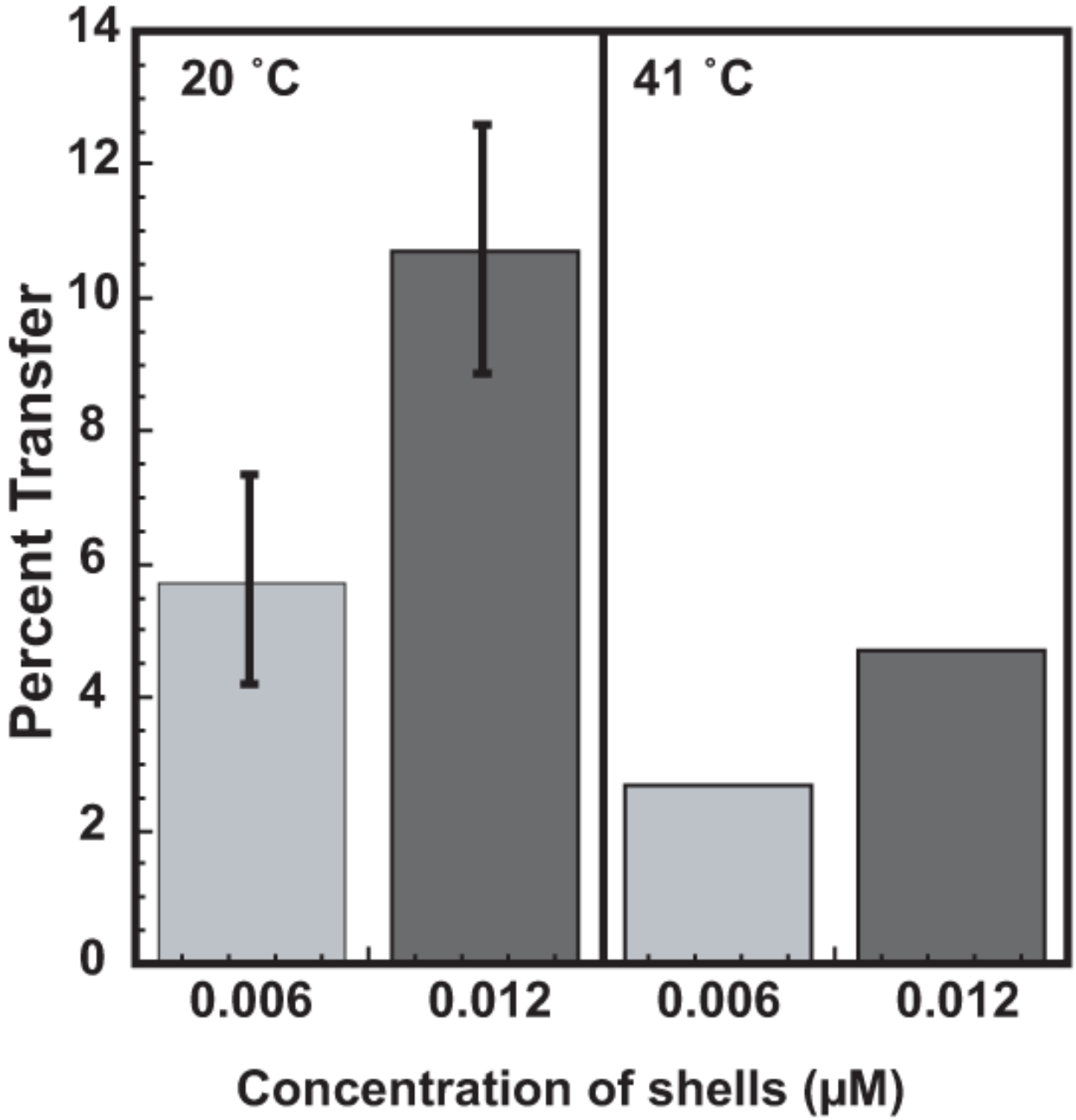

Figure 4. Radioactive monomers exchange with non-labeled shells

^{35}S-labeled coat protein monomers at 0.5 μM final were mixed with non-labeled coat protein shells at 0.006 and 0.012 μM shells. The samples were incubated at 20 °C and 41 °C for 1 day and separated by sucrose gradient sedimentation. The gradients were fractionated and the fractions were analyzed by liquid scintillation counting. The percent transfer was determined as described in the Materials and Methods. The error bars represent the standard deviation from 3 or 4 data sets